PCCP

Accepted Manuscript

This is an *Accepted Manuscript*, which has been through the Royal Society of Chemistry peer review process and has been accepted for publication.

Accepted Manuscripts are published online shortly after acceptance, before technical editing, formatting and proof reading. Using this free service, authors can make their results available to the community, in citable form, before we publish the edited article. We will replace this *Accepted Manuscript* with the edited and formatted *Advance Article* as soon as it is available.

You can find more information about *Accepted Manuscripts* in the Information for Authors.

Please note that technical editing may introduce minor changes to the text and/or graphics, which may alter content. The journal's standard Terms & Conditions and the Ethical guidelines still apply. In no event shall the Royal Society of Chemistry be held responsible for any errors or omissions in this *Accepted Manuscript* or any consequences arising from the use of any information it contains.

ROYAL SOCIETY OF CHEMISTRY

www.rsc.org/pccp

Please do not adjust margins

Journal Name

ARTICLE

Received 00th January 20xx,
Accepted 00th January 20xx

DOI: 10.1039/x0xx00000x

www.rsc.org/

Stability, Equilibrium Morphology and Hydration of ZrC (111) and (110) Surfaces with H_2O: A Periodic DFT and Atomistic Thermodynamics Study

Eric Osei-Agyemang,[a] Jean Francois Paul,[a] Romain Lucas,[b] Sylvie Foucaud,[b] Sylvain Cristol,[a†]

Abstract: ZrC is a non-oxide Ultra High Temperature Ceramic (UHTC) with excellent physical and mechanical properties used in nuclear plants and jet propulsion engines. However, mechanical properties can be lost because of the easy oxidation of its grain surfaces. One way of dealing with such problem is to coat the surface with inert carbides like SiC which can be grafted onto the ZrC surface by first modifying the exposed surfaces with reactive molecules. The stability of different terminations of the (111) facet was studied and the most stable is the termination on both surface layers by Zr atoms as it has been observed experimentally. A DFT calculation jointly with atomistic thermodynamic modelling has been used to study the reactivity of the (111) and (110) facets with H_2O. H_2O dissociates into surface hydroxyl groups with the release of H_2 and the OH groups preferentially adsorb at high surface coverage **(High adsorption energies at 1 ML coverage)**. The study of the adsorption of H_2O on the other low index surfaces allows the determination of the equilibrium morphology of the ZrC nanocrystallites in different environments. In vacuum, ZrC nanocrystallites reveal a cubic structure with much of the (100) surface and a small amount of the (111) facets at the corners. Hydration of the (111) surface was a strong process and hence water can be removed from the surface at temperatures above 1200 K at pressures lower than 10^{-9} bar while higher pressures of H_2 in the gas phase enhances removal of water. Wulff construction of the nanocrystallites after hydration indicates only the (111) surface at lower temperatures while revealing the (100) facets at higher temperatures. Thus whatever the experimental conditions, the (110) facet does not have to be considered.

I. Introduction

Zirconium Carbide (ZrC) is a high temperature non-oxide material which exhibits mixed covalent, ionic and metallic bonding characters. It is widely used in nuclear reactor linings, aerospace engines and in the manufacture of hard materials such as cutting tools. It is among the transition metal carbide (TMC) group of materials with high melting point (3430^{o}C). As it is a requirement for materials used in nuclear and aerospace industries to work in harsh environments, materials like high refractory ceramics are well suited.[1] As an example, nuclear plants with the future fourth generation engines are supposed to work at temperatures above 1200^{o}C. Hence these engines require materials with physic-chemical properties that are compatible with such working conditions.[2] According to its abovementioned properties, ZrC is a promising candidate for such applications. Working under severe conditions such as high temperatures and oxidizing environments is however not easily achieved due to the fact that introduction of a small dose of oxygen forms zirconium oxide layer on the surface[3] which leads to deterioration of the mechanical and other properties of the ceramic. Coating the surfaces with another ceramic material that is resistant to oxygen and maintains its physical properties at very high temperatures can help alleviate the oxidation problem.[4,5] Such coatings can be achieved by first modifying the ZrC surfaces with small molecules[6] in order to graft another material. In this context, the study of ZrC surfaces is of prime importance.

a. Unité de Catalyse et Chimie du Solide (UCCS), UMR-CNRS 8181, Université Lille 1, 59655 Villeneuve d'Ascq, Lille, France.
b. Laboratoire Science des Procédés Céramiques et de Traitements de Surface (SPCTS), UMR-CNRS 7315, Centre Européen de la Céramique, 87068 Limoges, France.

† Corresponding author: tel +33 320 43 45 03, fax +33 320 43 65 61; email sylvain.cristol@univ-lille1.fr
See DOI: 10.1039/x0xx00000x

Physical Chemistry Chemical Physics Accepted Manuscript

Please do not adjust margins

There are three distinct surfaces from the cubic structure of ZrC, (100), (110) and (111) surfaces to be considered. In addition to the most stable (100), the (111) surface is also of considerable stability[7] and has been prepared by many research groups.[8,9] Cleavage of the bulk ZrC crystal to form the (111) surface generates a surface which is either terminated by Zr layer or C layer. However, a recent Angle Resolved Photoemission Spectroscopy (ARPES) study has revealed the electronic structure of ZrC (111) surface is very similar to that of TiC, HfC, NbC and TaC (111) surfaces.[8] These other TMC (111) surfaces have been studied by Impact-Collision ion Scattering Spectroscopy (ICISS) and revealed that the first surface layer of these TMC's is terminated by metal layer.[10,11,12,13]

Furthermore, the preparation of the ZrC material is normally difficult to perform at conditions void of gaseous water molecules and as such the interaction of the individual surfaces with water is of paramount importance. Reactivity with water can lead to the formation of surface hydroxyl groups which will modify the chemical properties of the surfaces but can also be used as precursors for subsequent grafting of other materials onto the ZrC surface. There is however no extensive work, neither experimental nor theoretical on the reactivity of water with the ZrC (111) surface. The only experimental work performed on the reactivity of water on this surface is unpublished though mentioned in the paper by Noda et al.[8] Similarly, there is no report, neither experimental nor theoretical on the adsorption of molecules on the ZrC (110) surface even though a theoretical study on the surface energy has been carried out.[7]

In order to be able to determine the surface exposed by the ZrC crystallites in different environments and to construct crystal morphology, adsorption of water has been undertaken on these surfaces in order to obtain complete picture. The stability of the surfaces is studied with different terminations and different water coverage by means of periodic DFT calculations and atomistic thermodynamic modelling. Adsorption of water on the (100) surface which is also needed for constructing the equilibrium morphological shape is provided in a previous study.[14] The reactivity towards oxygen will be exposed in a subsequent paper.

The paper is divided as follows: section II describes the calculation scheme and structural models used for the current work while section III A provides the results for the calculated surface properties and description of the stability of the (111) surface with different terminations and its reactivity towards H_2O. Section III B provides results and description of the adsorption of H_2O on the (110) surface. Section III C provides details of charge analysis for hydration of the ZrC surfaces. In section III D, results and discussions on the equilibrium morphology of the bare nano-crystals as well as in hydrated environments at different temperatures are exposed. Finally, section IV draws conclusions on the current studies.

II. Calculation Scheme and Structural Models

All Calculations were performed using the Vienna Ab Initio Simulation Package (VASP)[15] which is based on Mermin's finite temperature DFT.[16] The electronic configurations used for Zr, O, H and C are [Kr]$4d^2 5s^2$, [He]$2p^6 1s^1$ and [He]$2s^2 2p^2$ respectively. PAW pseudopotentials[17] were used to replace the core electrons as well as the core part of the valence electrons wavefunctions in order to reduce the number of planewaves required to describe the electrons close to the nuclei. The Generalized Gradient Approximation (GGA) exchange correlation functional parameterized by Perdew, Burke and Ernzerhof (PBE),[18] was employed and the Methfessel-Paxton,[19] smearing scheme was used by setting the gamma parameter to 0.1 eV. The accuracy of the calculation results was evaluated by changing the energy cutoff from 200 eV to 600 eV while the k-point sampling mesh was evaluated from 2 x 2 x 2 to 11 x 11 x 11 using the standard Monkhorst-Pack,[20] special grids. From this evaluation, all subsequent bulk and surface calculations were performed by describing the valence electrons using the plane wave basis set with the cutoff of 500 eV while the integration of the Brillouin zone was performed with 9 x 9 x 9 k-points for the bulk and 9 x 9 x 1 k-points for surface calculations. The self-consistent field (SCF) procedure for resolution of the Kohn-Sham equations is assumed to be converged when energy changes of 10^{-4} eV between two successive iterations is reached. For bulk calculations, the positions of all ions were relaxed while for all surface calculations, the positions of all the ions in the three top most layers were relaxed in order to render the net forces acting upon them smaller than 10^{-2} eV/Å. The lattice parameter for the ZrC bulk was optimized by fitting the energy versus volume curve against the Murnaghan's equation of state as detailed in our previous work.[14]

According to the Fm3m space group of cubic ZrC, the non-equivalent, low index surfaces are (100), (110) and (111) surfaces as shown in figure 1. Their starting geometries were obtained by cleaving the optimized bulk structure along the corresponding normal directions. Unless otherwise stated, (1 x 1) surface unit cells were used for surface calculations In order to avoid surface-surface interactions; a vacuum of 12 Å was set as separation between two periodically repeated slabs.

For all calculations on the (111) surface, a (1 x 1) supercell was used with ϒ = 60° and an a parameter of 6.698 Å. This surface has an exposed area of 38.854 Å². The surface exposes four Zr atoms (figure 1). In all (110) calculations, a (1 x 1) supercell with a and b parameters of 4.736 Å and 6.698 Å respectively were used. This surface has an exposed area of 31.724 Å and consists of two Zr atoms and two C atoms (figure 1). The (110) surface slab is stoichiometric.

All surface calculations with adsorption of small molecules on the (110) surface were performed with at least 8 layer slabs and the three topmost layers were relaxed while keeping the remaining layers fixed to mimic bulk conditions. The surface

Physical Chemistry Chemical Physics Accepted Manuscript

energy for symmetric slabs with equivalent surfaces on both sides is computed as:

$$\gamma_{surf} = \frac{1}{2A}\left[E_{slab} - nE_{bulk}\right] \ldots\ldots\ldots\ldots\ldots eq.(1)$$

Where E_{slab} denotes the slab energy and nE_{bulk} is the energy of n ZrC units in the bulk structure (n being the number of ZrC units in the slab) while A is the surface area exposed by the surface planes.

Nine or ten atomic layers were used for the (111) surface stability calculations for stoichiometric and non-stoichiometric slab energy calculation and reactivity. The three outermost layers of the slab were allowed to relax while the remaining layers were kept fixed to mimic bulk properties. Cleaving of the ZrC (111) yields a stoichiometric slab with two inequivalent but complementary surfaces, one terminated with Zr layer and the other with C.

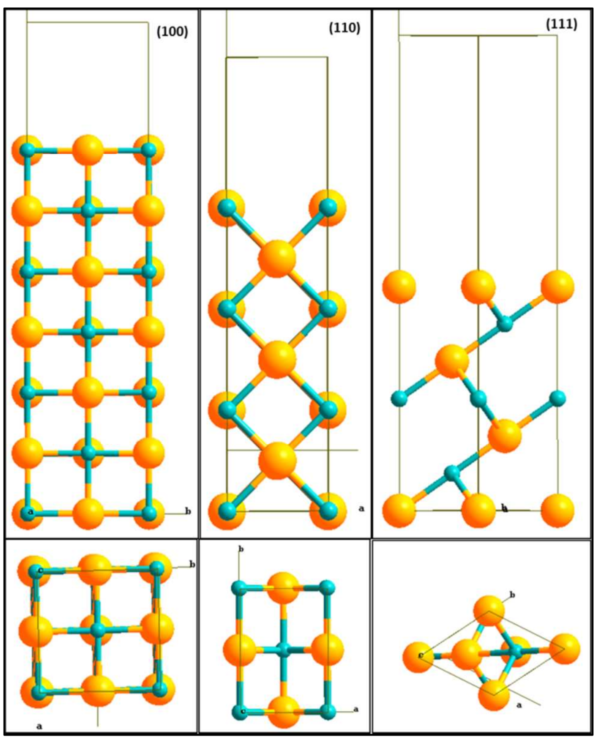

Figure 1. Different surfaces of ZrC. Upper Left (100), Upper middle (110) and Upper right (111) surfaces side view respec-tively. Bottom left, bottom middle, bottom right are (100), (110) and (111) top views respectively. Yellow = Zr, Blue = C

For these two inequivalent surfaces, the cleavage energy is calculated by computing the surface energies for symmetric slabs of terminating with the same atomic layer on both sides for each of the complementary surfaces. This enables estimation of the contributions made by each surface toward the cleavage energy. The surface energies for the two different surfaces are then added to obtain the cleavage energy.

The cleavage energy for the ZrC (111) surface with inequivalent surfaces (terminating with Zr on one surface layer and C on the other surface layer) is calculated using equation 2. [21]

$$E^{(Zr+C)}_{cleave} = \frac{1}{2A}\left[E^{Zr}_{slab} + E^{C}_{slab} - mE_{bulk}\right] \ldots\ldots\ldots eq.(2)$$

E^{i}_{slab} is the total energy of the symmetric slab with i termination, A the surface area, E_{bulk} the bulk energy per unit formula in the ZrC cubic structure and m is the total number of bulk formula units in the two slabs.

This mode of termination leads to the introduction of electrostatic forces in the slab due to the polar nature of the resulting slab. This polarity can be cancelled out by different modifications either with stoichiometric slabs, in which Zr or C atoms are displaced from one termination to the other or with non-stoichiometric slabs in which extra Zr or C atoms are added to the surfaces. The following nomenclature is used for the different terminations of the (111) surface in order to reduce the polarity of the surface slab. ***q*A-(111)-B*r*** is used as the notation where a layer of atom A terminates on one side of the slab and a layer of atom B terminates on the other side with *q* and *r* being the number of atoms A and B on both sides respectively. As an example, *2*C-(111)-*2*Zr means 2 C atoms are on one surface layer and 2 Zr atoms are on the other surface of the slab. The different surface terminations are shown in Figure 2. In order to account for the extra atoms in the slab, we used slabs which are symmetric with respect to the center of inversion.

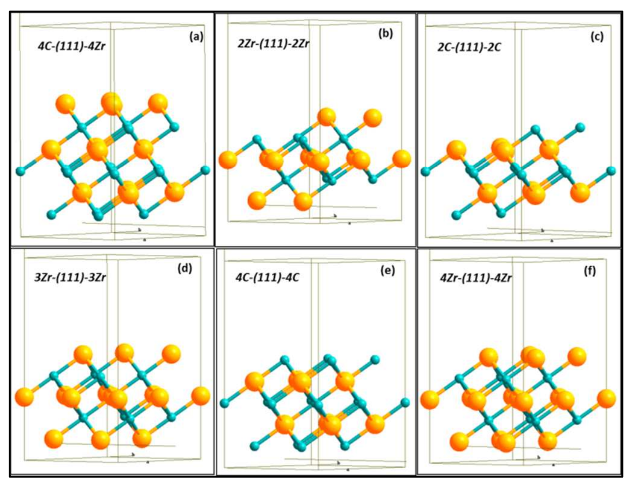

Figure 2. Different polar correction schemes used for the (111) surface. Stoichiometric structures (a, b, c) have the same number of Zr and C atoms while non-stoichiometric structures have excess of either Zr or C atoms in the structure.

Physical Chemistry Chemical Physics Accepted Manuscript

The SOWOS program[22] was used for prediction of the Wulff[23] shapes using the calculated surface energies for the (100), (110) and (111) surfaces in the absence and presence of water. The adsorption of water has been investigated in both an associative and a dissociative way by systematically testing different adsorption modes. The adsorption energies are then computed as:

$$E_{ads} = -[E_{surf-molecule} - E_{clean\,surf} - E_{molecule}] \ldots\ldots\ldots eq.(3)$$

$E_{surf\text{-}molecule}$ is the energy of the surface with the adsorbed molecule, $E_{clean\ surface}$ is the energy of relaxed clean surface and $E_{molecule}$ is the energy of the gaseous molecules. After obtaining the preferred adsorption modes, the effect of different coverage of the gaseous molecules was evaluated using 0.25 Monolayer (ML), 0.5 ML, 0.75 ML and 1 ML.

In all cases, the coadsorption of different number of water molecules were tested but the step by step adsorption process of one water molecule followed by another was observed to yield the most stable configurations. The step by step adsorption of water was finally used. The different coverages were defined by the number of available Zr sites on the surface. For the (111) surface, there are four Zr atoms and each site defines 0.25 ML. Moreover, for the (110) surface there are only two Zr atoms present and easy to define the 0.5 ML and 1 ML coverages. In order to obtain 0.25 ML and 0.75 ML, (2 x 1) super cells were used; revealing four Zr sites which makes it probable to define the 0.25 ML and 0.75 ML coverages.

Atomistic Thermodynamic Model

A thermodynamic treatment is needed to provide a more elaborate picture and explanations for the stability of the different surface structures. The appropriate surface property which can be used to account for the contribution of each surface termination to the cleavage energy is the surface grand potential, $\boldsymbol{\Omega}^i$.[21] This implies a contact with reservoirs of Zr and C. The surface grand potential of the i[th] termination is as follows:

$$\Omega^i = \frac{1}{2A}\left[E^i_{slab} - N_C\mu_C - N_{Zr}\mu_{Zr}\right] \ldots\ldots\ldots eq.(4)$$

N_C and N_{Zr} are the number of C and Zr atoms in the surface slab while μ_c and μ_{zr} are the carbon and zirconium chemical potentials respectively. A is the surface area of the (111) termination. Since the chemical potentials of C and Zr are not independent because they are assumed to be in equilibrium with bulk ZrC, they are related through the expression: $\mu_{ZrC} = \mu_C + \mu_{Zr}$. μ_{ZrC} is the chemical potential of the bulk ZrC unit formula and it is approximated by the total energy for bulk ZrC unit formulae E^{bulk}_{ZrC}. Substituting this into equation 4 yields:

$$\Omega^i = \frac{1}{2A}\left[E^i_{slab} - N_{Zr}E^{bulk}_{ZrC} + \mu_C(N_{Zr} - N_C)\right] \ldots\ldots\ldots eq.(5)$$

Since it has already been established that the synthesis process of ZrC is accompanied with excess of graphite carbon,[6] we define equation 5 in terms of the chemical potential of carbon. The chemical potential of C is defined relative to the chemical potential of C in its standard state and hence $\Delta\mu_C = \mu_C - \mu_C^*$ where μ_C^* is the chemical potential of C in its reference state and is calculated as the bulk energy of graphite Carbon E^{bulk}_C. Substituting the expression of $\Delta\mu_C$ into equation 5 yields the surface grand potential as:

$$\Omega^i = \frac{1}{2A}\left[E^i_{slab} - N_{Zr}E^{bulk}_{ZrC} + E^{bulk}_C(N_{Zr} - N_C) + \Delta\mu_C(N_{Zr} - N_C)\right] \ldots\ldots\ldots eq.(6)$$

If we make the following definition:

$$\gamma_i = \frac{1}{2A}\left[E^i_{slab} - N_{Zr}E^{bulk}_{ZrC} + E^{bulk}_C(N_{Zr} - N_C)\right] \ldots\ldots eq.(7)$$

Substituting equation 7 into equation 6 yields:

$$\Omega^i = \gamma_i + \frac{1}{2A}\left[\Delta\mu_C(N_{Zr} - N_C)\right] \ldots\ldots\ldots eq.(8)$$

Where γ_i is the surface energy of the selected (**i = *q*A-(111)-B*r***) termination as defined in equation 1. Thus the surface grand potential Ω^i is made up of the surface energy contributing part as well as the dependence and contribution of each atom on the surface.

Using equation 8, a range of accessible Ω^i can be obtained if we have the minimum and maximum $\Delta\mu_{Zr}$ and $\Delta\mu_C$. It is assumed that the Zr and C form do not condensate on the ZrC (111) surface. To obtain the maximum Zr and C chemical potentials, the chemical potential of each of the species must be lower than the energy of the atom in the stable bulk phase of the considered species and hence:

$$\begin{cases} \Delta\mu_C = \mu_C - E^{bulk}_C < 0 \\ \Delta\mu_{Zr} = \mu_{Zr} - E^{bulk}_{zr} < 0 \end{cases} \ldots\ldots\ldots\ldots eq.(9)$$

Where $\Delta\mu_C$ and $\Delta\mu_{Zr}$ are the relative values of the different chemical potentials with respect to E^{bulk}_C and E^{bulk}_{Zr} which are the energies of C in graphite and Zr in hcp zirconium bulk metal respectively. By combining $\mu_{ZrC} = \mu_C + \mu_{Zr}$ with the

Physical Chemistry Chemical Physics Accepted Manuscript

This journal is © The Royal Society of Chemistry 20xx

expression for $\Delta\mu_{Zr}$ and $\Delta\mu_C$ in equation 9, we obtain the lower boundary for the Zr and C chemical potentials as:

$$\begin{cases} \Delta\mu_C > E^f_{ZrC} \\ \Delta\mu_{Zr} > E^f_{ZrC} \end{cases} \dots\dots\dots\dots\dots eq.\ (10)$$

Where E^f_{ZrC} the formation energy for bulk ZrC is, computed using the equation $E^f_{ZrC} = E^{bulk}_{ZrC} - E^{bulk}_{zr} - E^{bulk}_{C}$ and we calculated it as -1.59eV. A plot of the surface grand potential Ω^i against the range of chemical potential values obtained is then used to explain the thermodynamic stability of the different terminations. Thus the surface grand potential accounts for both stoichiometric and non-stoichiometric slabs. It is obvious from equation 6 that, for stoichiometric and symmetric surfaces, the third and fourth terms in the equation becomes zero and the expression reduces to surface energy while the cleavage energy is calculated as twice the surface energy. The surface grand potential is therefore the equivalent surface energy for both non-stoichiometric and stoichiometric slabs.

In order to establish relationship between the calculations performed and experimental working conditions, we used the already well-established atomistic thermodynamic scheme,[24] where the surface and the adsorbed molecule are assumed to be in equilibrium with the gas phase which serves as a reservoir. This then allows for the definition of the adsorption Gibbs free energy *($\Delta_r G$)* as a function of thermodynamic parameters such as temperature, T and pressure, P using the general equation:

$$\Delta_r G = \left[\, \Delta E_O + E_{ZPE(surf-molecule)} - \Delta \sum n\, \mu(T,\ p) \,\right] \dots eq.(11)$$

$\Delta\sum n\mu(T,\ p)$ is the difference in chemical potential of the reactant and product gas phase molecules. $\Delta E_o = [E_{el\ (surface\text{-}molecule)} + E_{el\ (released\ specie)} - E_{el\ (surface)} - n\ E_{el(molecule)}]$ is the difference in electronic energy of the considered surface and the small molecules according to the following process:

ZrC surface + n (molecule) ↔ ZrC surface-[n (molecule)] + released specie.....................eq (12)

The ΔE_o is also the adsorption energy E_{ads} in equation 3.
The adsorption of the gas phase molecules unto the surface affects the chemical potential of the gaseous molecules due to frustrations of the rotational degrees of freedom as compared to the gas phase and consists of a temperature dependent term [$\Delta\mu^o\ (T)$] and a pressure dependent term.

$$\Delta\mu(T,P) = \Delta\mu^o(T) + RT\ln\left(\frac{P}{P^o}\right) \dots\dots\dots eq.(13)$$

The temperature dependent term can however be computed with statistical thermodynamics as below:

$$\Delta\mu^o(T) = \left[\, E_{ZPE} + E_{vib(0\to T)} + E_{rot} + E_{trans} \,\right] + RT - T(S_{vib} + S_{rot} + S_{trans}) \dots\dots eq.(14)$$

These thermal contributions are introduced by the loss of rotational and translational degrees of freedom upon adsorption of the small molecules onto the surface as well as the change in the vibrational contribution. The values of $\Delta\mu^o(T)$ at different temperatures are obtained using standard statistical thermodynamic formulas with equilibrium geometry and calculated frequencies. A value of P^o of 1 atm was used and a plot of *($\Delta_r G$)* against pressure P was obtained at different constant temperatures. The lowest of such plots is the most stable system in a given experimental conditions.
The surface energy, γ_{hkl} (H_2O), as a function of the n adsorbed water molecules at different temperatures can be calculated using the equation

$$\gamma_{hkl}(H_2O) = \frac{1}{2n}\left[\gamma^o_{hkl} + \theta_{hkl}\Delta_r G_{hkl}(P,T,n)\right] \dots\dots eq.(15)$$

With $\Delta_r G_{hkl}(P,\ T,\ n) = \Delta E_o + E_{ZPE(surface\text{-}molecule)} - \Delta\sum n\ \mu(T,p)$, $\theta_{hkl} = 2n/A_{hkl}$ is the surface coverage by water, A_{hkl} is the surface area of the exposed hkl plane, γ^o_{hkl} is the surface energy of the bare surface (θ_{hkl} = 0). The calculated $\gamma_{hkl}(H_2O)$ values were then used to predict the Wulff morphological structure of the ZrC nanoparticles at specified temperature and pressure. The Wulff shapes have been calculated using a water partial pressure of 0.01 bar.

III. Results and Discussion

A. ZrC(111) Surface

Surface Structure Properties of ZrC(111). The calculated surface and cleavage energies for the different polar correction schemes are summarized in Table 1 and compared to the value of the polar surface (Figure 2, *4*C-(111)-*4*Zr).

Table 1. Calculated surface energies γ_i as in equation 7 with different polar correction schemes for ZrC (111) surface (Figure 2). For symmetrically equivalent slabs, cleavage energy is calculated as twice the surface energy

	Surface energy		*Cleavage energy*	
Surface termination	γ_{rigid}/ me.VÅ^{-2}	$\gamma_{relaxed}$/ me.VÅ^{-2}	γ_{rigid}/ me.VÅ^{-2}	$\gamma_{relaxed}$/ me.VÅ^{-2}
4C-(111)-4Zr	-	-	638.6	597.7
2Zr-(111)-2Zr	287.7	236.6	575.4	473.2

Please do not adjust margins

Physical Chemistry Chemical Physics Accepted Manuscript

2C-(111)-2C	265.15	233.3	530.3	466.6
3Zr-(111)-3Zr	229.6	190.7	459.2	381.4
4C-(111)-4C	444.0	428.8	888	857.6
4Zr-(111)-4Zr	194.6	168.9	389.2	337.8

Both relaxed and unrelaxed surface energies are reported. The comparison of the computed surface energies γ_i reveals that the structure in which both surface layers are covered with four Zr atoms; ***4Zr-(111)-4Zr*** is by far the most stable with the lowest surface grand potential within the range of C chemical potentials. It has been observed experimentally that there is always an excess of carbon in ZrC samples in the form of graphite[6] and hence the corrections made for the non-stoichiometric structures are done with bulk energy of carbon in graphite as in equation 7. The calculated surface energy for this stable surface (Zr terminated on both sides) is **168.9meV/Å^2.** Arya and Carter[7] reported a value of 151.5 meV/ Å^2 for the ZrC (111) metal terminated surface. However, for the non-stoichiometric slabs, the authors used a correction that took into account only the number of atoms and not their chemical nature. As such it is difficult to compare the two surface energies. The relative stability of this (111) surface with the (100) and (110) surfaces is however consistent with the conclusions drawn by the authors. Comparing the cleavage energy of this termination with the as-cleaved (111) surface; *4*C-(111)-*4*Zr there is a high gain in stability. The thermodynamic stability plot of the surface grand potential against the chemical potential of carbon showing the stability regions of the different surface terminations is shown in figure 3. Thus at all carbon chemical potentials $\Delta\mu_C$ only the structure with 4 Zr atoms terminated on both sides is thermodynamically stable. We also provide in figure 3, the surface grand potentials for the (100) and (110) surface for comparisons.

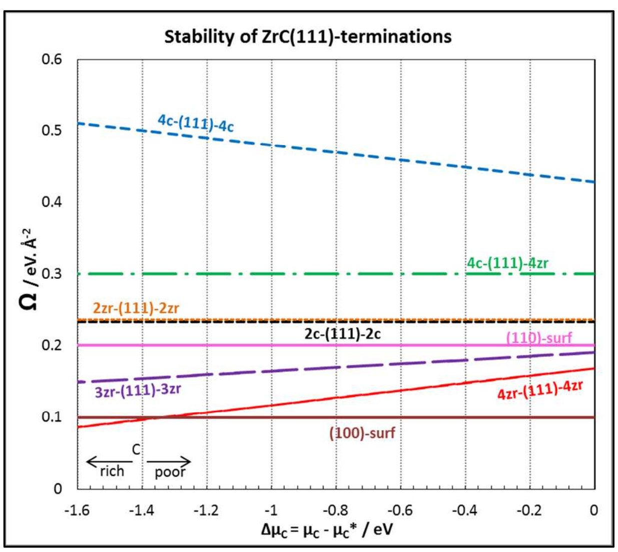

Figure 3. Surface grand potential of (111) surface terminations at different Zr chemical potentials

For stoichiometric surfaces, the surface grand potential expression reduces to the surface energy. We predict that at low C chemical potentials $\Delta\mu_C$ < - 1.32 eV, the *4*Zr-(111)-*4*Zr surface termination is even more stable than the (100) surface. It can also be observed from table 2 that all surface structures with carbon layer terminations yield extremely high surface energies and hence are not stable. The experimentally observed layer of Zr termination[25] is therefore corroborated by our stability studies. We selected the most stable structure ***4Zr-(111)-4Zr*** for our subsequent calculations.
The calculated surface energies for the ZrC (111) polar surfaces are summarized in Table 2 in comparison with the values for the (110) and (100) surfaces.

Table 2. Calculated surface energies (in meV.Å^{-2}) for ZrC surface planes. γ_{rigid} is surface energy for rigid slab and $\gamma_{rel.}$ is surface energy for relaxed slab. Ref. is reference

surface	γ_{rigid}	γ_{rel}	*Ref. / γ_{rigid}*	*Ref./γ_{rel}*
(100)	105.7	99.6	105 [7]	99.4[7], 101[26], 96.8[27]
(110)	218.4	200.4	213 [7]	199.7 [7]
4Zr-(111)-4Zr	194.6	168.9	174.7[7]	151.5[7]

This structure, which has four Zr atoms terminating both surface layers was then further optimized and used for calculation of the density of states (DOS). The total DOS (TDOS) and the projected DOS (PDOS) onto the atoms are shown in Figure 4. A comparison of the TDOS with that of the bulk structure shows a significant introduction of new surface states at the Fermi level (E_f), arising from Zr-d and Zr-p states. The metallic nature of the surface is evidenced and due mostly of the Zr-d occupied surface states at the Fermi level. The Zr d – C p mixing region arises at lower energies. Thus the very high electronic states observed for the (111) surface suggest a high reactivity of this surface compared to the (100) surface.[7]

Physical Chemistry Chemical Physics Accepted Manuscript

 This journal is © The Royal Society of Chemistry 20xx

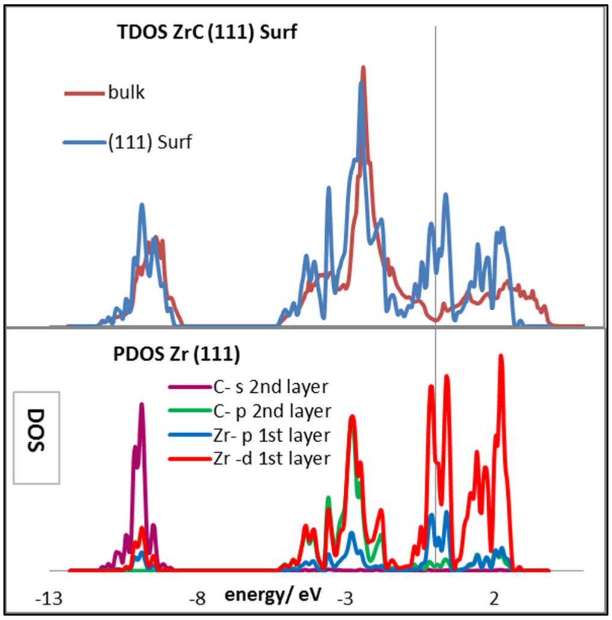

Figure 4. **TDOS and PDOS of ZrC (111) Surface**

There is no surface reconstruction of the relaxed ZrC bare (111) surface. It was observed that the interlayer spacing between the first and second layers is reduced while the second interlayer spacing increases substantially. The bond distance between the first and second layer, d_{1Zr-2C} which is the distance between Zr in first layer and C in second layer is 2.24 Å and agrees well with values calculated by other groups, 2.22 Å,[27] and the second interlayer spacing between C in second layer and Zr in third layer d_{2C-3Zr} = 2.45 Å. The other interlayer spacing and bond distances approach that of bulk.

Reactivity of H_2O on Bare ZrC(111) Surface. After testing with different configurations, the most stable form of adsorption was used to compute the adsorption energies E_{ads}. The adsorption process was carried out in a stepwise manner, starting with one H_2O molecule, then two H_2O molecules and so on. Both associative and dissociative modes of adsorption were tested. The adsorption energy was then calculated for successive water additions and as averages for different coverages of the (111) surface. All adsorption processes on the (111) surface is observed to favor complete dissociation into atomic species which sites at fcc three-fold hollow site just above Zr atoms in the third or fifth layers.

1 H_2O molecule Adsorption: The observed reaction of a single H_2O molecule is a complete dissociation process where H_2O dissociates into atomic O and H species which adsorbs very strongly at fcc three fold hollow sites between three surface Zr atoms. This is accompanied by a very strong energy of adsorption, $\mathbf{E_{ads} = 4.58}$ **eV**. **Moreover, a calculation was made to ascertain the subsequent combination of the two adsorbed H atoms to form H_2 and release into the gas phase. This reaction was found to be endothermic.** **O-(111)-2H ↔ O-(111) + $H_{2\ (gas)}$, ΔE_{rxn} = 1.33 eV**. The complete dissociation mode of adsorption is shown in figure 5a1 and 5a2.

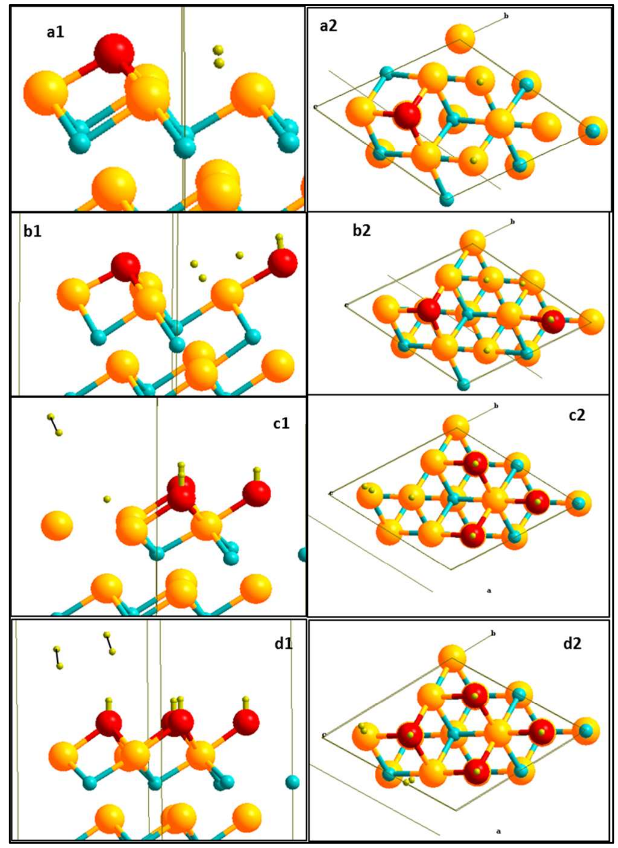

Figure 5. **Side view (left) and top view (right) for dissociation of water on ZrC (111) surface with 1, 2, 3 and 4 H_2O molecules. Blue(C), yellow(Zr), red(O), light green(H)**

The calculated bond distances between the O and surface Zr atoms were 2.36 Å, 2.15 Å and 2.15 Å while that of H and the surface Zr atoms are between 2.15 Å and 2.20 Å.

2 H_2O molecules adsorption: In the presence of two H_2O molecules, there is a mixed mode of adsorption. There is a combination of complete and partial dissociation of H_2O molecules. This can be viewed us a process where the first H_2O molecule dissociates completely into O and H atoms, occupying three of the available four fcc hollow sites while the second water molecule dissociates partially into surface OH group adsorbing at the remaining fcc hollow site and the H atom adsorbs at an fcc hollow site above Zr atom in the fifth layer. The consecutive adsorption of the second H_2O molecule is accompanied by a high adsorption energy, $\mathbf{E_{ads} = 3.25}$ **eV**. Thus even though the complete dissociation into atomic species has a very high adsorption energy, the partial dissociation also has a high energy. Figure 5b1 and 5b2 shows the complete and partial dissociation of 2 H_2O molecules on ZrC (111) surfaces. The calculated bond distances between the

Physical Chemistry Chemical Physics Accepted Manuscript

Please do not adjust margins

Please do not adjust margins

surface O and Zr atoms are 2.170 Å, 2.21 Å and 2.10 Å, between O of OH group and surface Zr atoms are 2.37 Å, 2.22 Å and 2.42 Å while those between the H atoms and surface Zr atoms are between 2.003 Å and 2.663 Å.

3 H_2O molecules adsorption: Adsorption of three H_2O molecules resulted in partial dissociation into surface hydroxyl groups with the release of H_2 molecules. In the subsequent addition of the third H_2O molecule, there is the formation of three surface OH groups and H specie all adsorbing at fcc three fold hollow sites with the release of H_2 molecule. The successive adsorption of the third H_2O molecule is associated with an adsorption energy, **E_{ads} = 1.22 eV**. **This somehow low adsorption energy as compared to one and two H_2O molecule adsorption may be due to the lateral repulsion between the three adsorbed OH species on the surface.** Figure 5c1 and 5c2 shows the adsorption of three molecules on (111) surface with the release of H2 into the gas phase. The measured bond distances between O of OH group and the surface Zr atoms are in the range of 2.00 Å and 2.36 Å. The bond distances between the adsorbed H atom and the surface Zr atoms were 2.24 Å, 2.24 Å and 2.24 Å.

4 H_2O molecules adsorption: The adsorption of four H_2O molecules on the (111) surface leads to adsorption at all possible fcc three fold hollow sites on the surface plane. There is the partial dissociation of H_2O molecules to form four OH groups adsorbing at the four available fcc sites with the release of two H_2 molecules into the gas phase. This adsorption process is governed by the equation: ZrC(111) + $4H_2O \leftrightarrow$ ZrC(111)-4(OH) + $2H_2$. The final geometry of adsorbed surface species are shown in figures 5d1 and 5d2. The adsorption energy for the successive addition of the fourth H_2O molecule, **E_{ads} = 1.14 eV**. This value is lower than that for adsorption of three H_2O molecules as part of the reaction energy is used in releasing two H_2 molecules into the gas phase. The calculated average bond distance between the surface Zr atoms and the O atom of the OH group is 2.37 Å. At this point, the surface is saturated with the maximum number of H_2O molecules as all the possible adsorption sites are occupied.

A complete picture of the potential energy surface showing all the adsorption process of water and the release of H_2 is shown in figure 6. This aids in easy visualization of the reaction process.

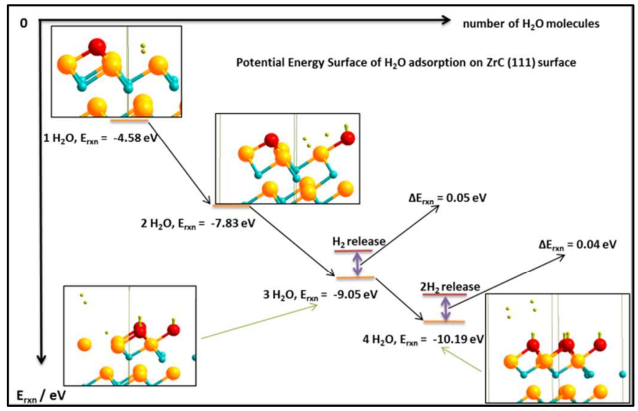

Figure 6. Potential energy surface of H_2O adsorption on ZrC (111) surface. Blue(C), yellow(Zr), red(O), light green(H)

The calculated TDOS and PDOS of the fully hydroxylated (111) surface is shown in figure 7. A comparison of the TDOS (figure 7 top panel) of the clean and hydrated surfaces shows attenuation of the surface states around the Fermi level as well as introduction of a new band at around -5.5 to -7.0 eV due to the surface OH groups.

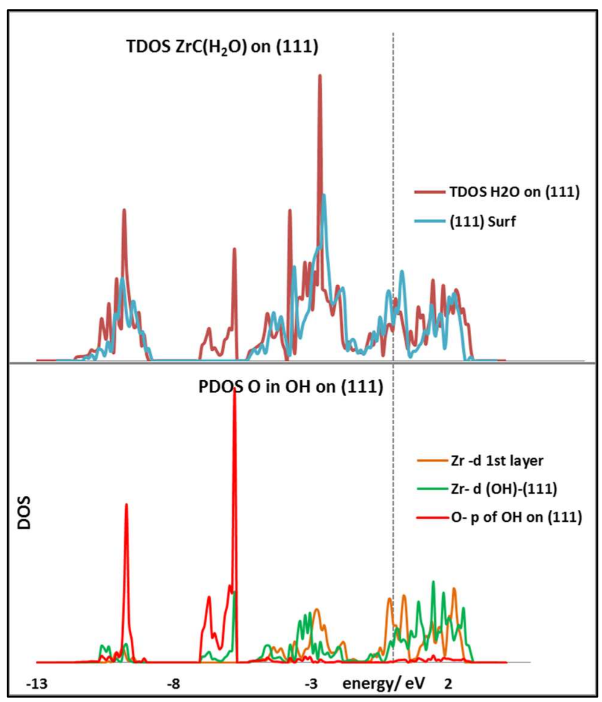

Figure 7. TDOS and PDOS plots for dissociation of four water molecules on ZrC (111) surface into OH and release of H_2 (full coverage). Violet legend: clean (111) surface

Since H_2 is a released gas, it has no effect on surface DOS and hence it is not shown. A projection of the DOS (figure 7 bottom) onto the O atom of the hydroxyl group shows

Physical Chemistry Chemical Physics Accepted Manuscript

This journal is © The Royal Society of Chemistry 20xx

Please do not adjust margins

attribution of the new state to the OH group. This is in good agreement with what is observed experimentally where the OH band is observed at ~ -7.0 eV.[8] This band is attributed to the 1π state of OH group. Moreover, the unoccupied bands are shifted to higher energies as they interact with O- p electrons. The PDOS (figure 7 bottom panel) of the surface Zr atoms shows a considerable decrease in the surface d states and the newly observed band has a high contribution from the surface Zr d states. This shows a significant mixing of the metal- d and O- p from OH group, yielding stable surface hydroxyl groups accompanied by high adsorption energy.

A summary of the successive adsorption energies of different amount of H_2O molecules added to the surface as well as the calculated average adsorption energies per H_2O molecule at different water coverage on the (111) surface is provided in table 3. These values show a decrease in the adsorption energies towards higher coverages as a result of the removal of H_2 into the gas phase.

Table 3. Adsorption Energies, Eads for different coverage of H_2O on (111) surface

Coverage	*0.25 ML*	*0.50 ML*	*0.75 ML*	*1.0 ML*
Eads/ per H_2O/ eV	*4.58*	*3.81*	*2.95*	*2.50*
Successive Adsorption Energies of H2O				
Number of H_2O	*1*	*2*	*3*	*4*
Eads/ eV	*4.58*	*3.25*	*1.22*	*1.14*

These calculated adsorption energies were then used to obtain thermodynamic stability plots using calculated Gibbs free energy of adsorption values at low and high temperatures. Due to hydrogen released by the hydration process, the stability plots are obtained as functions of both H_2O and H_2 pressures at different temperatures. This type of plot is very useful when there is the need to remove surface hydroxyl groups to achieve the bare surface as hydrogen can be introduced to the system to drive the equilibrium to the left side of the reaction to produce water.

Plots of six different temperature regimes are provided (Figure 8). **This phase diagram is obtained as follows: at each temperature, the Δ_rG value is calculated for different pressures of oth H_2 and H_2O gases at different coverages. The surface coverage which has the lowest Δ_rG value at a selected partial pressure of H_2 and H_2O is the most stable. The different coverages at different pressure combinations are then used to obtain the stability plots for different temperatures.**

At lower temperatures between 200 and 400 K, the surface is fully covered with OH groups at all H_2O and H_2 pressures considered. As the temperature is increased to 500 K, small regions of the 0.5 ML begin to appear. This region is characteristic at H_2 pressures above 10^{-1} bar and H_2O pressures below 10^{-8} bar. The 0.5ML is a mixture of partial and complete dissociation of H_2O molecules into surface O atoms and OH species. At 700 K, there is desorption of two H_2O groups at 10^{-9} to 10^{-10} bar of H_2O at H_2 pressures of 10^{-2} to 1 bar while three H_2O groups are desorbed from the surface at all H_2 pressures at 10^{-10} bar of H_2O. At 1000 K, a small region of the 0.5ML coverage still appears while there is a significant increase in the 0.25ML region. The bare surface is recovered at higher temperatures above 1200 K at very low pressures of H_2O. At 1500 K, the bare surface is still recovered at H_2O pressures below 10^{-10} bar at all H_2 pressures while the 0.5ML phase is totally lost. If only water molecules are introduced in the feed (without external addition of H_2), only the lower region of the diagram below the diagonal line Figure 8 can be reached. This shows that partial or total surface dehydration can only be achieved at very high temperature.

It has to be noted that, the 0.75ML coverage is not stable at all studied temperatures for all the combinations of H_2 and H_2O partial pressures considered as the adsorption energies of the third and fourth water molecules are similar.

Physical Chemistry Chemical Physics Accepted Manuscript

Please do not adjust margins

Journal Name

ARTICLE

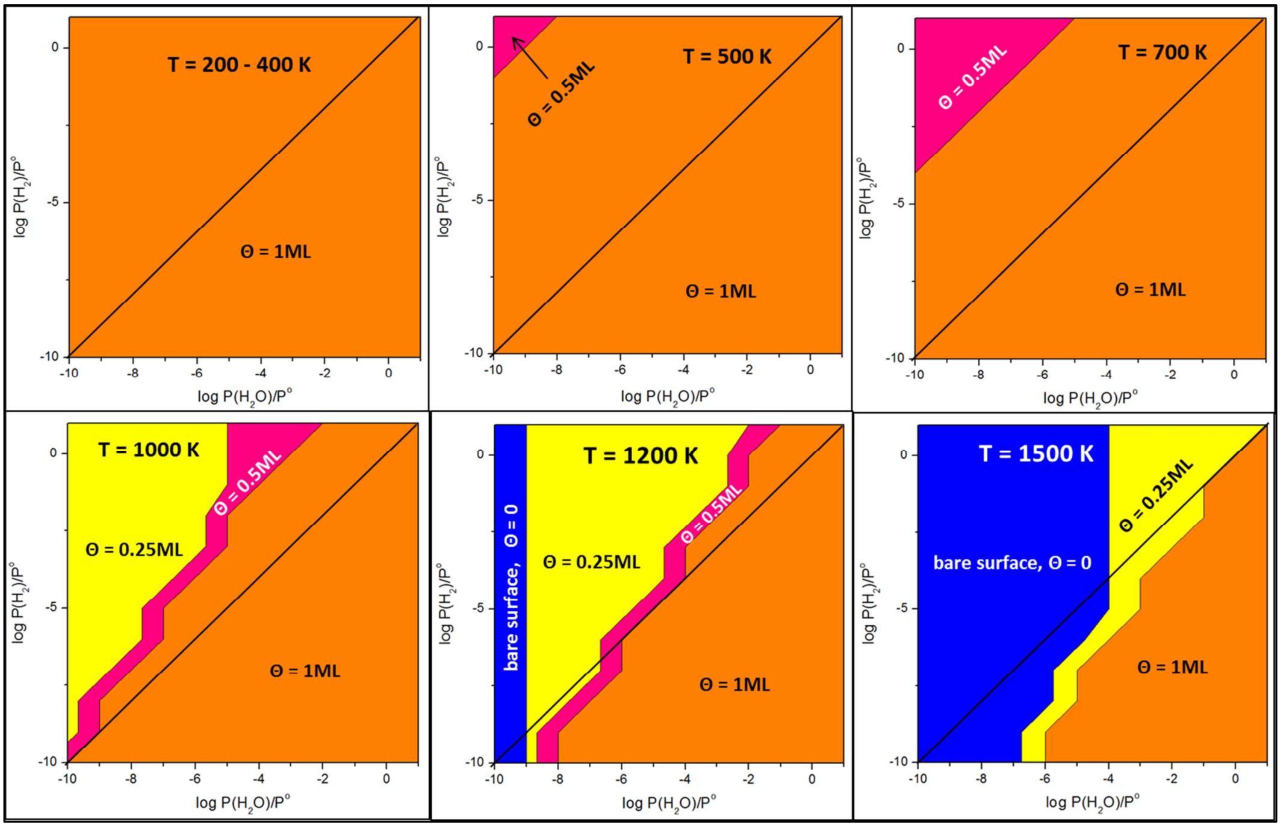

Figure 8. 2D- stability plot for H_2O adsorption on ZrC(111) surface at different temperatures. The 0.75ML coverage is not stable at all studied partial pressures of H_2 and H_2O at all temperatures.

B. ZrC (110) Surface

Surface Structure of ZrC(110) Surface. The ZrC (110) surface structure was studied after full relaxation of the three topmost surface atom layers. There is no surface reconstruction after relaxation. The relaxation energy from the rigid surface is very small as compared to the (111) surface. Zr atoms of the first and second layers relaxed inwards while C atoms of the first and second layers relaxed upwards. Both the Zr –Zr and C –C bond distances of the surface layer remain the same as that of the bulk (3.35 Å). The first layer relaxes inwards while the second layer relaxes outward. The vertical distance between the C of the first layer and C of the third layer decreases from 3.35 Å to 3.27 Å (d_{1C-3C} = 3.27 Å) and d_{2C-3C} = 2.33 Å. The vertical distance between Zr of the second layer and Zr of the fourth layer increases from 3.35 Å to 3.36 Å ($d_{2Zr-4Zr}$ = 3.36 Å). Thus surface relaxation causes an elongation of the Zr –C bonds between the second and third layers with the distance between Zr of the second layer and C of the third layer being d_{2Zr-3C} = 2.39 Å while the distance between C of the second layer and Zr of the third layer is d_{2C-3Zr} = 2.45 Å (the value in bulk ZrC is 2.37 Å). There is however a decrease in these inter-layers distances as one move from the second layer to the first layer. The resulting d_{1Zr-2C} = 2.21 Å and the d_{1C-2Zr} = 2.30 Å.

The high surface energy of the (110) surface is reflected in the TDOS as compared to that of the bulk (Figure 9). Creating of the (110) surface from the bulk structure introduces a significant amount of new surface states just above the Fermi level. These new states are made of Zr d and C p orbitals. These new surface states are accounted for by the reduction in the coordination numbers of the surface Zr and C atoms to 3 as compared to coordination of 6 in the third and subsequent lower layers.

Physical Chemistry Chemical Physics Accepted Manuscript

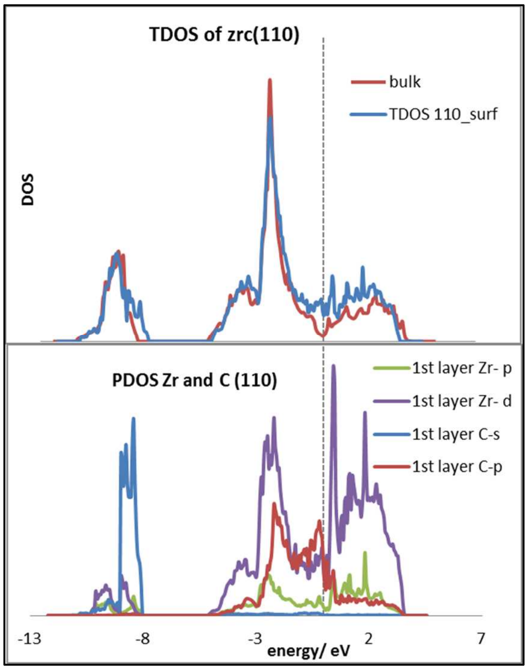

Figure 9. TDOS and PDOS of ZrC (110) surface

H2O Adsorption on ZrC (110) Surface: Hydration of the (110) surface was also carried out in a successive fashion of H_2O molecule addition to the surface. The most stable form of adsorption of H_2O on this surface is adsorption of O containing species as a bridge between two surface Zr atoms and on top of C atom in the third layer whereas H atoms adsorbed on top of surface C atoms.

***1 H_2O molecule**:* The first H_2O molecule led to complete dissociation of water into atomic oxygen as a bridge between two Zr atoms and the resulting H atoms adsorbing on top of the two surface C atoms. This mode of adsorption yielded an adsorption energy, $\mathbf{E_{ads} = 4.22\ eV}$. The adsorption mode is shown in Figure 10a1 and 10a2. The calculated bond distances between the O atom and the surface Zr atoms is 2.028 Å while the distances between the H atoms and the surface C atoms is 1.113 Å.

***2 H_2O molecules**:* Adsorption of a second H_2O molecule led to partial dissociation of H_2O molecules into surface hydroxyl groups and H atoms. Thus two surface OH groups are formed as bridges between two surface Zr atoms and on top of the two available C atoms in the third layer as shown in figures 10b1 and 10b2. This adsorption of the second H_2O molecule was accompanied by a lower adsorption energy, $\mathbf{E_{ads} = 3.13\ eV}$ as compared to the adsorption energy of one H_2O molecule. At this point, the full surface coverage is achieved as all the stable adsorption sites are occupied. The calculated bond distances between the O atoms of the surface OH groups and the surface Zr atoms are within the range of 2.23 Å and 2.25 Å while those between the adsorbed H atoms and the surface C atoms is 1.12 Å. A (2 x 1) supercell was used to further obtain the adsorption energies for the 0.25ML and 0.75ML coverages which were calculated to be **4.21 eV** and **3.44 eV** per water molecule respectively.

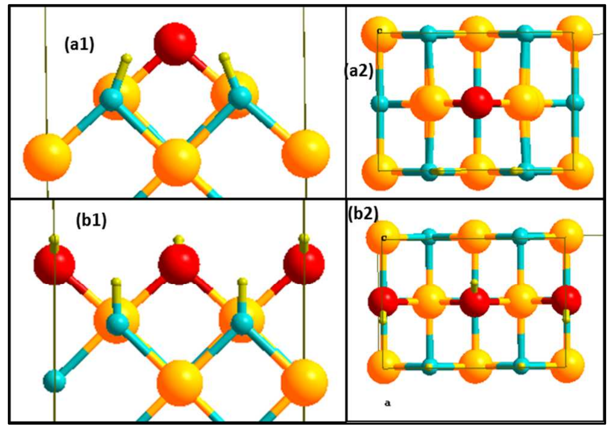

Figure 10. Adsorption of H_2O on ZrC(110) surface. Left(side view), right(top view), blue(C), yellow(Zr), red(O), light green(H)

The TDOS and PDOS of the partial dissociation of H_2O into surface hydroxyl groups are shown in figure 11. The TDOS shows the OH features appearing at about -7.5 eV which falls within the experimentally observed position range for the OH group.[8]

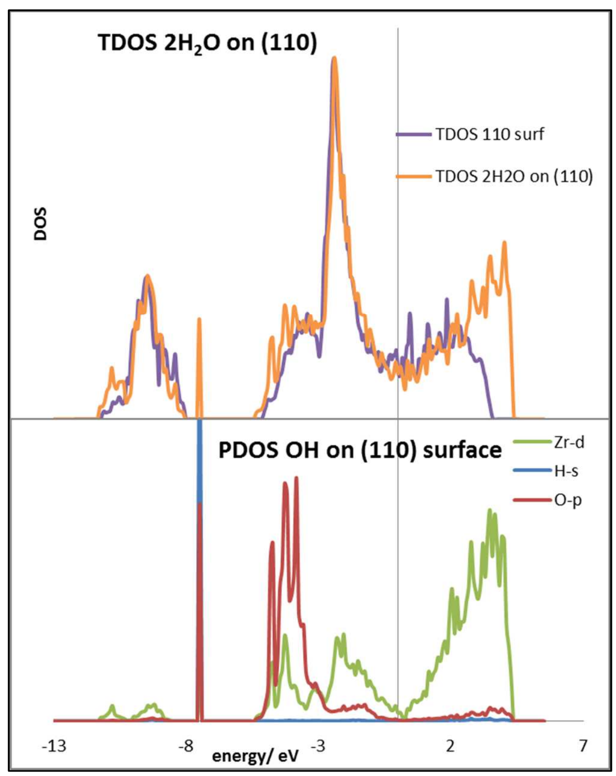

Please do not adjust margins

Physical Chemistry Chemical Physics Accepted Manuscript

[Figure 11](#). TDOS and PDOS of H_2O adsorption on ZrC (110) surface, green legend: Zr on surface layer

There is a slight attenuation in the surface states around the Fermi level upon adsorption of the OH groups and the PDOS shows a mixing of the Zr d orbitals with the O p orbitals during the adsorption of the OH groups on the surface. There is also a large increase of the Zr d band above the Fermi level as the surface is hydrated.

Examination of the adsorption energies at different coverage of water ([Table 4](#)) shows strong adsorption at lower coverages.

[Table 4](#). Adsorption Energies, E_{ads} for different coverage of H_2O on (110) surface

Coverage	*0.25 ML*	*0.50 ML*	*0.75 ML*	*1.0 ML*
E_{ads}/ per H_2O/ eV	*4.21*	*4.22*	*3.44*	*3.13*

The adsorption energies at different coverages were then used to obtain the thermodynamic stability plot in [Figure 12](#). **This stability plot was obtained in a similar manner as that of figure 8**. A 2D diagrams is provided to aid easy viewing and interpretation. The full coverage of the surface with hydroxyl groups is achieved at low temperatures between 200 and 500 K at all H_2O partial pressures considered whereas the 0.5ML phase which is made up of atomic O and H species on the surface is stable between 500 and 1000 K at low partial pressures of H_2O below 10^{-5} bar.

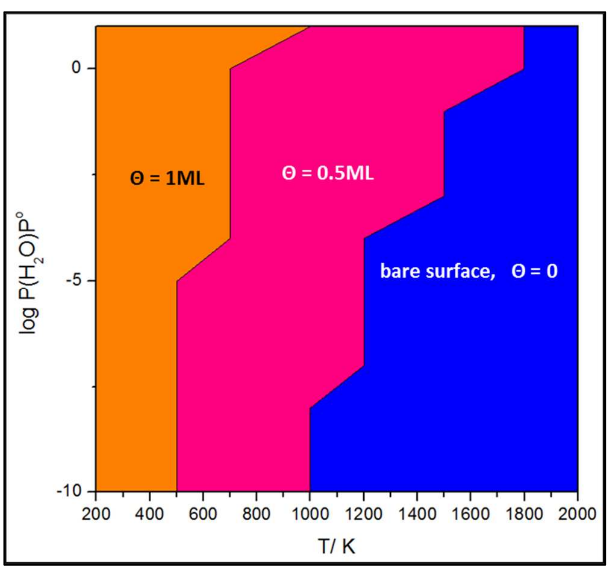

[Figure 12](#). 2D surface stability plot for H_2O adsorption on ZrC(110) bare surface at different partial pressures of H_2O. 0.75ML coverage is not stable at all studied temperatures and partial pressures of H_2O.

It is also stable at higher temperatures up to 1800 K but at higher pressures of H_2O above 10^{-3} bar. The bare surface is recovered at temperatures above 1000 K at a wide range of H_2O partial pressures. It can easily be noted that, both the 0.25ML and 0.75 ML phases are not stable.

C. Characterization of Surface Oxidation

An analysis of oxidation of surface Zr and C atoms were carried out using the Bader code developed for VASP.[28] This was carried out for both the clean ZrC (110) and (111) surfaces. In order to provide a more complete picture of comparison, the same analysis was carried out on the adsorption of molecular water on the (100) surface.[14] [Table 5](#) provides a summary of the Bader charge analysis.

[Table 5](#). Bader Charge analysis for Zr and C atoms for clean and hydrated ZrC surfaces[a]

Parameter	*ZrC-(100)*	*ZrC-(110)*	*ZrC-(111)*
	Clean Surface		
Net Q_C	*-1.62*	*-2.27*	*-1.84*
Net Q_{Zr}	*1.65*	*2.47*	*1.09*
	Hydrated Surface		
	H_2O-(100)	*HO-(110)*	*HO-(111)*
ΔQ_{Zr}	*0.06*	*0.27*	*0.68*
ΔQ_C	*0.05*	*0.51*	*0.05*
ΔQ_O	*-0.11*	*-0.22*	*-0.15*

[a] The variation of the net charges (*ΔQ_{Zr} and ΔQ_C*) is defined with respect to the charges on Zr and C in the clean ZrC surfaces while *ΔQ_O* is defined with respect to the charge of O in H_2O gas. The charge analysis was carried out using 1ML coverage for both the (110) and (111) surfaces while 0.5 ML coverage was used for the (100) surface.

In case of hydration of the (100) surface with molecular water, there is clearly no change in the electron density of the surface Zr atoms as can be seen in [table 5](#). Moreover, upon hydration of the (110) surface, there is small charge transfer from the surface Zr atoms to O atoms and from surface C atoms to the attached H atoms. In case of the (111) surface, upon hydration with the release of gaseous H_2, a clear a redox process is evidenced and with a significant oxidation of surface Zr atoms (*ΔQ_{Zr} = 0.68 electron*) [table 5](#).

D. Equilibrium morphology of nano crystallites

Physical Chemistry Chemical Physics Accepted Manuscript

This journal is © The Royal Society of Chemistry 20xx

The equilibrium morphological shape of the ZrC nano crystallites are predicted for the bare surface as well as the hydrated surfaces at a range of selected temperatures.

Bare Surface: The computed surface energies of the (100), (110) and the (111) surface (Zr-terminated) were used to predict the equilibrium Wulff morphology of the ZrC nanocrystallites in the absence of reactive molecules. The predicted Wulff structure is depicted in Figure 13. The predicted morphology shows only the presence of the (100) and (111) surfaces and the (110) surface does not appear. The crystallite structure is that of a cube with small (111) facet at the corners which represents less than 1% of the exposed total surface area of the ZrC nanocrystallites. This is in excellent agreement with what has been observed experimentally as only the (100) surface is normally easily observed.[29]

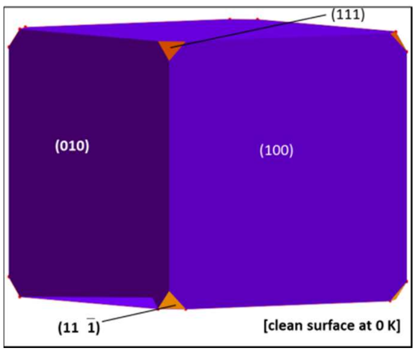

Figure 13. Predicted Wulff solid for bare ZrC nanocrystallites

H_2O adsorption: Adsorption of water on the (100) surface resulted in dissociative mode into surface OH groups on Zr atoms and H on surface C atoms with adsorption energy of 1.0 eV. Details of H_2O adsorption on the (100) surface is provided in our previous paper.[14] A complete list of the **surface energies** of the individual facets of ZrC with their relative abundances upon hydration at different temperatures is compiled in Table 6. For the (111) surface, there is a very strong interaction with water which provides much stability that over compensates the surface energy of the bare facets at low temperatures and hence negative surface energies upon adsorption of water are reported. Thus the (111) is highly stabilized relative to the other surfaces upon hydration in the range of 200 K to 500 K temperatures as shown in table 6. This also reveals that the (110) surface is not present as compared to the other facets upon hydration of the nano crystallites. The calculated surface energies at different temperatures after hydration were then used to obtain the Wulff construction of the equilibrium morphology of the nanocrystallites as shown in Figure 14.

Table 6. Surface free energies of the exposed hydrated surface planes of ZrC at various temperatures with their relative abundances (in bracket) for $P(H_2O)/P^o$ = 0.01 bar and $P(H_2)/P^o$ = 0.005 bar.

Surface energy/ meV/Å²	*200 K*	*300 K*	*400 K*	*500 K*
$\gamma_{(100)}(H_2O)$	43.0 (0%)	63.4 (0%)	84.5 (0%)	99.6 (0%)
$\gamma_{(110)}(H_2O)$	27.6 (0%)	42.1 (0%)	57.3 (0%)	73.0 (0%)
$\gamma_{(111)}(H_2O)$	-73.3 (100%)	-58.7 (100%)	-43.5 (100%)	-27.7 (100%)
Surface free energies at higher temperatures				
	700 K	*1000 K*	*1200 K*	*1500 K*
$\gamma_{(100)}(H_2O)$	99.6 (0%)	99.6 (12.3%)	99.6 (35.1%)	99.6 (76.4%)
$\gamma_{(110)}(H_2O)$	105.8 (0%)	144.6 (0%)	162.5 (0%)	190.3 (0%)
$\gamma_{(111)}(H_2O)$	5.1 (100%)	56.9 (87.7%)	92.9 (64.9%)	147.0 (23.6%)

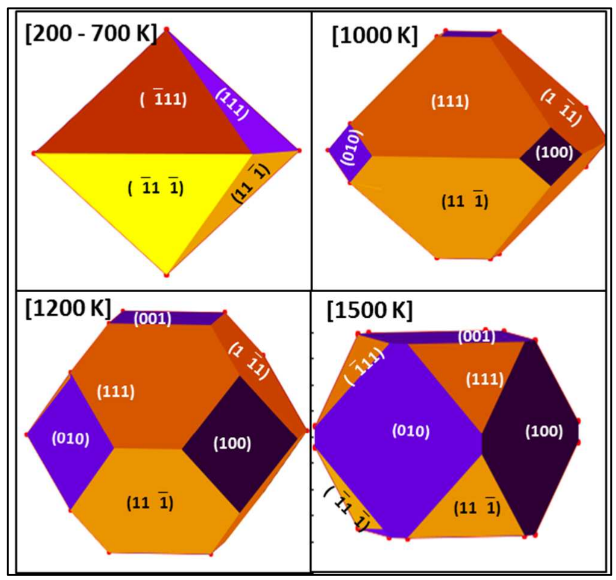

Figure 14. Equilibrium Wulff shapes of hydrated ZrC at different temperatures. The (100) facets shown are bare surfaces while (111) are all shown for 1 ML full coverage which is the most stable at the chosen temperatures

This construction was done at 0.01 bar H_2O pressure and 0.005 bar H_2 pressure. From 200 to 700 K, only the (111) facets are observed. This is due to the high stability of the (111) facets by four OH groups and subsequently stabilized further by the release of H_2 gas molecules. At 1000 K, 12 percent of the (100) surface is revealed as a result of removal of some OH groups from the (111) surface and the subsequent comparison in the resulting surface energies of the already bare (100) surface and the partially hydroxylated (111) facets. The surface energy for the (100) surface increases from 200K to 500K and remains

Physical Chemistry Chemical Physics Accepted Manuscript

fairly constant thereafter because at the lower temperature the surface is stabilized by the weakly adsorbed OH groups upon hydration, characterized by the low adsorption energy of the OH groups.[14] Thus at lower temperatures of 200K to 700K the extremely low surface free energy (negative values for surface energies) of the (111) surface results in smaller sized crystals. Moreover, at higher temperatures, the stabilizing OH groups are removed and the bare surface is exposed, resulting in an increased surface energy.

At 1200 K, more OH groups are removed from the (111) surface and the bare (100) surface increases in abundance to 35 percent with the (111) surface being 65 percent. As the temperature is increased further to 1500 K, the (111) facets decrease significantly in abundance while 76% of the surfaces is now made of the (100) facets. At all these temperatures, the full coverage with OH on the (111) surfaces are the most stable the 0.01 bar H_2O pressure and 0.005 bar H_2 pressure used while all (100) facets which appear are the bare surfaces. It can be clearly seen that at all temperatures, the (110) facets are not revealed. In order to functionalize the ZrC surfaces with hydroxyl groups which can be obtained on the (100) facets or (111) facets, one can work at a wide range of temperatures and pressures and still achieve this aim. Thus there appear some changes in the morphology of the ZrC nanocrystallites when the surfaces are hydrated at different temperatures.

Summary and conclusion

DFT and atomistic thermodynamic modelling have been combined to study the stability of ZrC (111) surfaces with different terminations of carbon atoms and zirconium atoms in an attempt to get rid of polarity in the slab. All cases tested yielded the most stable surface as the one with four Zr atoms in confirmation with experimental observations. The calculated surface energies of the different facets were then used to obtain the equilibrium morphology of the ZrC nanocrystallites in clean environments in vacuum. The equilibrium morphology at 0 K revealed the nano crystallites as cubes exposing much of the (100) surface with truncations at the corners due to the appearance of small amounts of the (111) facets and no (110) facets.

We have also studied the adsorption and reactivity processes of water on the (110) and (111) surfaces. A study of the adsorption of H_2O on the (111) and (110) surfaces was carried out and we observed complete dissociation into hydroxyl groups and release of hydrogen molecules for the (111) surface. There is however complete dissociation into oxygen as a bridge between two surface zirconium atoms with the dissociated hydrogens sitting on top of surface carbon atoms at low coverage for the (110) surface while higher coverage results in surface hydroxyl groups. Thermodynamic stability plot shows the monolayer coverage with surface OH species as the most stable at a wide range of pressures until about 10^{-5} bar at 1200 K before the bare (111) surface is recovered. However, on the (110) surface the full coverage with OH and H atoms are stable at lower temperatures while the 0.5ML coverage is stable between 700 K and 1000 K. The bare (110) surface is achieved at temperatures above 1000 K and lower H_2O partial pressures. Construction of the equilibrium morphology shows that from 200 to 1500 K temperature, the ZrC surfaces can be functionalized with surface hydroxyl groups, specifically on the (111) surface.

Acknowledgements

Numerical results presented in this paper were carried out using the regional computational cluster supported by Université Lille 1, CPER Nord-Pas-de-Calais/FEDER, France Grille, and CNRS. We highly appreciate and thank the technical staff of the CRI-Lille 1 center for their strong and helpful support. The project is supported by Agence Nationale de la Recherche under Contract No. ANR-12-BS08-004-02 (CollZSiC: Elaboration de nanocomposites coeur/coquille ZrC/SiC).

References

1. L. E. Toth, *Transition metal carbides and nitrides*, Academic press, New York, 1971.
2. D. Gosset, M. Dollé, D. Simeone, G. Baldinozzi and L. Thomé, *Journal of Nuclear Materials*, 2008, **373**, 123-129.
3. H. Li, L. Zhang, L. Cheng and Y. Wang, *Ceramics International*, 2009, **35**, 2277-2282.
4. H. Li, L. Zhang, L. Cheng, Y. Wang, Z. Yu, M. Huang, H. Tu and H. Xia, *Journal of the European Ceramic Society*, 2008, **28**, 887-891.
5. P. Greil, *Advanced Engineering Materials*, 2000, **2**, 339-348.
6. M. Iijima and H. Kamiya, *The Journal of Physical Chemistry C*, 2008, **112**, 11786-11790.
7. A. Arya and E. A. Carter, *Surface Science*, 2004, **560**, 103-120.
8. T. Noda, M. Yamazaki, K. Ozawa, K. Edamoto and S. Otani, *Surface Science*, 2000, **450**, 27-33.
9. T. Noda, T. Nakane, K. Ozawa, K. Edamoto, S. Tanaka and S. Otani, *Solid State Communications*, 1998, **107**, 145-148.
10. A. Masakazu, O. Chuhei, Z. Shigeaki, O. Shigeki and I. Yoshio, *Japanese Journal of Applied Physics*, 1981, **20**, L829.
11. W. Hayami, R. Souda, T. Aizawa, S. Otani and Y. Ishizawa, *Surface Science*, 1992, **276**, 299-307.
12. W. Hayami, R. Souda, T. Aizawa, S. Otani and Y. Ishizawa, *Physical Review B*, 1993, **47**, 13752-13758.
13. R. Souda, T. Aizawa, S. Otani and Y. Ishizawa, *Surface Science*, 1990, **232**, 219-227.
14. E. Osei-Agyemang, J. F. Paul, R. Lucas, S. Foucaud and S. Cristol, *The Journal of Physical Chemistry C*, 2014, **118**, 12952-12961.
15. J. Hafner, *Journal of Computational Chemistry*, 2008, **29**, 2044-2078.
16. N. D. Mermin, *Physical Review*, 1965, **137**, A1441-A1443.

Physical Chemistry Chemical Physics Accepted Manuscript

This journal is © The Royal Society of Chemistry 20xx

Please do not adjust margins

17. G. Kresse and D. Joubert, *Physical Review B - Condensed Matter and Materials Physics*, 1999, **59**, 1758-1775.
18. J. P. Perdew, K. Burke and M. Ernzerhof, *Physical Review Letters*, 1996, **77**, 3865-3868.
19. M. Methfessel and A. T. Paxton, *Physical Review B*, 1989, **40**, 3616-3621.
20. H. J. Monkhorst and J. D. Pack, *Physical Review B*, 1976, **13**, 5188-5192.
21. F. Bottin, F. Finocchi and C. Noguera, *Physical Review B*, 2003, **68**, 035418.
22. D. Scopece, *Journal of Applied Crystallography*, 2013, **46**, 811-816.
23. G. Z. Wulff, *Z.Kristallogr.*, 1901, **34**, 449-530.
24. K. Reuter and M. Scheffler, *Physical Review Letters*, 2003, **90**, 461031-461034.
25. Y. Hwang, T. Aizawa, W. Hayami, S. Otani, Y. Y. Ishizawa and S.-J. Park, *Surface Science*, 1992, **271**, 299.
26. J. Li, D. Liao, S. Yip, R. Najafabadi and L. Ecker, *Journal of Applied Physics*, 2003, **93**, 9072-9085.
27. A. Vojvodic, C. Ruberto and B. I. Lundqvist, *J Phys Condens Matter*, 2010, **22**, 375504.
28. W. Tang, E. Sanville and G. Henkelman, *Journal of Physics: Condensed Matter*, 2009, **21**, 084204.
29. G. Mathieu, Ph.D, Universite de Limoges, 2010.

Physical Chemistry Chemical Physics Accepted Manuscript